Aeroacoustic study of a simplified wing-flap system in generic configurations

B. Lemoine and M. Roger

LMFA, Ecole Centrale de Lyon, 36 avenue Guy de Collongue, Bât. KCA, 69130 Ecully, France
benoit.lemoine@ec-lyon.fr

Airframe noise produced by the high-lift devices of an aircraft significantly contributes to noise exposure around airports. The VALIANT project supported by the EC with this in mind is aimed at providing a reliable experimental database as well as to assess numerical and theoretical models predicting far-field levels and directivity. In this context, the proposed paper is about the interaction of a flat-plate wing and a non-lifting airfoil. Aerodynamic and acoustic measurements performed for several configurations (various streamwise and transverse distances, flow speeds and incident turbulence rates) are described. An original analytical model in an overlapping configuration is developed, based on the half-plane Green's function with uniform flow and an iterative scattering procedure.

1 Introduction

According to a recent report from ODESA [4] (Observatoire De l'Environnement Sonore de l'Aéroport Lyon Saint-Exupéry), aircraft noise generated at landing is about 5 dB higher than at take-off. Then, it is known that airframe noise is the dominant component of sound-generation during approach, especially because of high-lift devices which are fully deployed. High-Lift Device (HLD) noise involves intricate sound-generating and sound-scattering mechanisms due to association of different solid surfaces in close vicinity of each other embedded in a flow. However, these physical mechanisms are not still well understood.

Therefore, a simplified wing/flap system is studied to characterize interactions between the two bodies. Experimental investigations first lead to the characterization and the behaviour of the flow around them by several aerodynamic tests. Then, far-field acoustic measurements bring information about spectral content and directivity of the studied configurations. Then, an original model is aimed at studying overlapping configurations with a uniform flow. An iterative procedure is proposed, releasing the compactness hypothesis which is usually assumed in most of the analytical models in the literature. Few results are finally introduced in comparison with experiments.

2 Experimental investigations

2.1 Set-up description

Two series of experiments have been carried out in the anechoic open-jet wind-tunnel of the Centre Acoustique at ECL (France). The mock-ups are constituted of two parallel bodies installed at zero angle of attack in order to focus the study on interactions between the wing and the flap and to avoid complex flow mechanisms due to real geometries that could produce sound (figure 1). The wing is a NACA0012-ended flat plate with a chord of 0.6 m and a thickness of 15 mm. It is shifted in the nozzle by 0.2 m to avoid pressure fluctuations due to the impact of the flow with the wing-plate leading-edge. The flap – a NACA0012 airfoil with a chord of 0.1 m – can be moved in close vicinity around the wing-plate trailing-edge. Both bodies are fixed by two brush-ended plates so that installation noise is reduced by about 5 dB. About 10 relative arrangements of the two bodies are possible. Configurations 1 and 2 correspond to a flap in the wake of the wing-plate, whereas the others are overlapping arrangements with various d and h parameters that respectively correspond to the overlapping length and the transverse distance as shown in figure 5. Moreover, the configuration 0 is defined as a *no œap* configuration, *id est* when the wing-plate is alone. This reference configuration especially leads to the deduction of the flap contribution in the total noise. However, results obtained for configuration 4 only are shown in this article, so as to focus the interest on an overlapping configuration. The values of d and h for this configuration are 20 mm and 15 mm respectively.

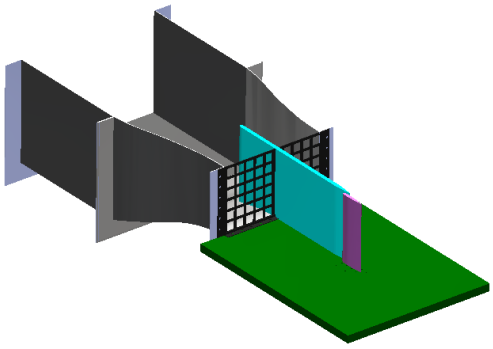

Figure 1: CAD of the experimental setup. Configuration 4 with turbulence grid installed at the nozzle outlet.

Two inflow conditions have been investigated: a *clean* inflow where the turbulence rate is under 0.5%, and a *turbulent* inflow where the turbulence rate is about 7% is generated by adding a grid at the nozzle outlet. The flow speed varies from 30 to 100 m/s with most of the investigations done at 50 m/s. Aerodynamic and acoustic measurements have been carried out mainly focussed on configurations 0, 2 and 4 (EC-project VALIANT configurations for comparisons). Three aerodynamic tests were performed on the one hand – single hot wire anemometry, steady-state and fluctuating wall-pressure – and two acoustic tests on the other hand – far-field directivity and source localization. The latter is not addressed here.

2.2 Tests overview

The flow characteristics are measured by a single hot-wire anemometry technique in order to estimate the turbulence rates as well as the mean and fluctuating velocity profiles in the studied area (around the wing-plate trailing-edge). The resulting mean profiles in configuration 4 are shown in figure 2. For both inflow conditions, the boundary-layer reaches 10 mm near the wing trailing-edge. In *clean* inflow, the boundary-layer which develops on the pressure-side of the wing-plate seems to merge on the suction-side of the flap, whereas it is still important when the inflow is highly turbulent. Furthermore, the wake of the wing is deviated towards the flap pressure-side because of its interaction with the flap boundary layer. It is finally interesting to point out that the flow in the channel between the two bodies is accelerated because of the convergent-divergent nozzle geometry of the channel. Few spectra were also obtained at various points that validate the turbulent characteristics with a $^{-5}/_{3}$-slope decrease as Von Karmán energy spectrum.

Fluctuating wall-pressure has been measured using the Remote Microphone Probe (RMP) technology developped at

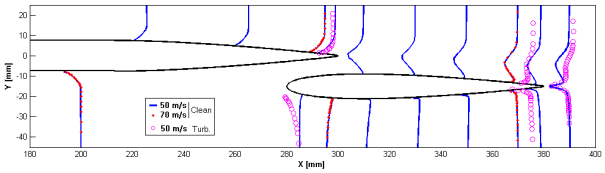

Figure 2: Normalized transverse mean velocity profiles in configuration 4. Clean inflow at 50 m/s (-) and 70 m/s (•), turbulent inflow at 50 m/s (○).

ECL [10]. This is a quasi non-intrusive technology that allows the heavy instrumentation to be outside the jet, by capturing the pressure fluctuations at the body surface through holes of diameter 0.5 mm connected to B&K $^1/_4$-inch microphone membrane by a capillary tube inside the mock-up. Most of the 36 probes are located in the horizontal mid-span plane in order to avoid wall effects of the installation, the others are along the span to get spanwise coherence. Once corrected by the frequency response function of the probe, the wall-pressure power spectral density (PSD) is calculated for each probe. Figure 3 represents the effect of the two inflow conditions on the PSD on the wing-plate suction-side surface (Fig 3-a) and the flap pressure-side surface (Fig 3-b). The flap behaves in the same way for both flow conditions with a higher wall-pressure level in turbulence case. In contrast, the wing-plate spectrum – high-frequency main contribution – appears to transition to broadband pattern similar to flap spectrum. No peak or tone is put in evidence.

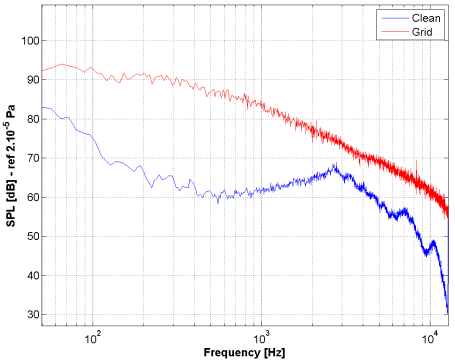

(a)

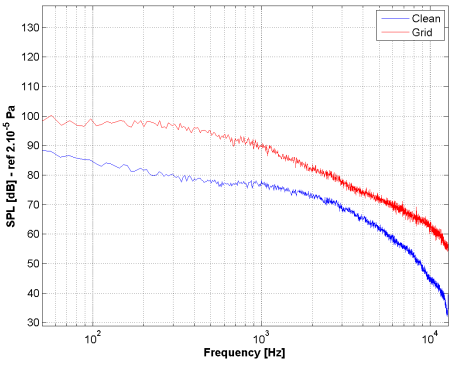

(b)

Figure 3: Comparison of wall-pressure PSD at 50 m/s for both inflow conditions. (a) Wing-plate pressure-side surface. (b) Flap suction-side surface.

The steady-state wall-pressure is also measured using the RMP holes and pressure gauges instead of microphones. The pressure coefficient is then calculated around the mock-ups. Weak variations of C_p around zero confirm the non-lifting behaviour of the bodies in the flow although a slight increase is formed at the flap leading-edge, due to vicinity of the wing-plate and turbulent boundary-layer impingement.

The far-field directivity has been measured using two opposite B&K $^1/_2$-inch microphones mounted on an automatically rotating two-arm system – each arm has a length of 1.8 m – where the rotation center fits with the axis of the set-up and the wing-plate trailing-edge. Measurements are made every 5° from 45° to 135°. Spectra are averaged on 30 blocks with a sampling frequency of 25.6 kHz. Moreover, the shear-layer refraction corrections proposed by Amiet and Schlinker [3, 12] are accounted for. Colour maps of noise level against angle and frequency are then plotted as shown in figure 4. From this kind of graph, directivity patterns can be obtained by integrating an horizontal spectral bandwidth of the map, whereas the spectrum for each angle corresponds to a vertical cross-section. An asymmetrical behaviour is typically found for this arrangement because of overlapping (asymmetrical) configuration, even though the gap is much smaller than the microphone distance (ratio ≈ 120). By subtracting the wing-alone contribution it is possible to deduce the flap contribution map. A large signature extent with upstream radiation is formed for low-frequencies and higher frequencies seem to mainly radiate downstream, both with interference fringes.

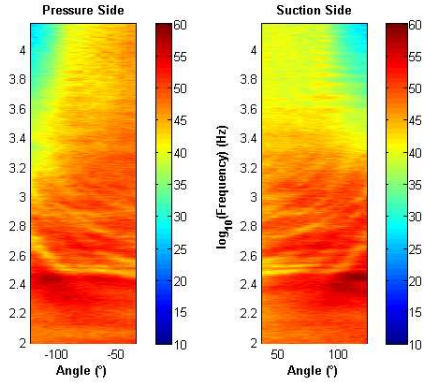

Figure 4: Colour map of far-field acoustic level against angle and frequency. Flap contribution at 50 m/s. (left) Pressure-side. (right) Suction-side.

Source localizations have also been performed by ONERA at ECL site, using an *in-house* cross-shape antenna of 109 B&K $^1/_4$-inch microphones. A classical beamforming was used for post-processing. The first results showed that the whole set-up had no significant parasitical effect on the far-field measured noise.

3 Analytical improvement for overlapping configurations

3.1 Problem statement

The generic configuration for analytical modelling is shown in figure 5. The wing is assumed a rigid half-plane and the flap a thin rigid strip of infinite span and chord length c. The fluid is moving uniformly at flow speed U_0 along the chordwise direction e_1 normal to the transverse direction e_2. The

unit vector e_3 is pointing upwards from what would correspond to the suction-side of the wing, opposite to the vertical shift of the flap. This gap is noted h and the horizontal shift d is defined between the wing trailing-edge and the flap leading-edge.

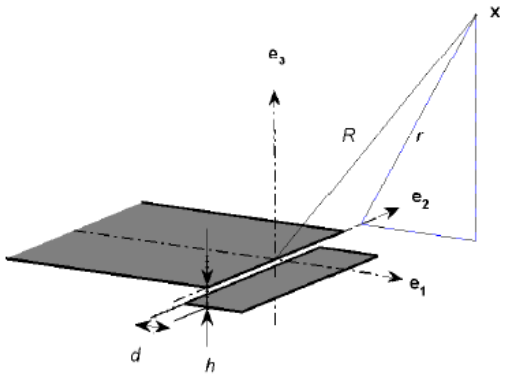

Figure 5: Generic wing-flap configuration and reference frame. The overlap is defined by negative values of the horizontal shift d when referred to the scattering edge.

According to the classical statement of linearized unsteady aerodynamic theories in the frequency domain, the presence of the flap in the incident disturbed flow results in an additional disturbance potential ϕ' solution of the convected Helmholtz equation

$$\beta^2 \frac{\partial^2 \phi'}{\partial x_1^2} + \frac{\partial^2 \phi'}{\partial x_2^2} + \frac{\partial^2 \phi'}{\partial x_3^2} + 2ikM_0 \frac{\partial \phi'}{\partial x_1^2} + k^2 \phi' = 0 \qquad (1)$$

with $\beta^2 = 1 - M_0^2$, assuming a time dependance $e^{-i\omega t}$. The impingement of turbulence on the flap leading-edge needs being addressed only for an isolated oblique gust of amplitude $\tilde{w}(k_1, k_2)$ with chordwise and spanwise wavenumbers $k_1 = K_1 = \omega/U_0$ and k_2 respectively.

It is then assumed homogeneous boundary conditions in e_2-direction to reduce the expression of $\phi' = \phi(x_1, x_3)\, e^{ik_2 x_2}$. Consequently, the problem can be solved using two-dimensional version of the half-plane Green's function. The passage to three-dimensional version can be done by Oberai's transposition procedure [9].

Original Amiet's problem of the response of a flat-plate airfoil to an incident velocity gust [2] is a reduction of the global problem described above, from which the scattering half-plane is removed. Reissner's transformation is used to obtain a standard Helmholtz equation

$$\Phi = e^{-iM_0^2 k_1^* y_1^*/\beta^2} \qquad \beta^2 = 1 - M_0^2$$
$$y_{1,2}^* = 2\frac{y_{1,2}}{c} \qquad y_3^* = 2\beta\frac{y_3}{c}$$
$$k_{1,2}^* = \frac{k_{1,2} c}{2} \qquad k_1 = \frac{k}{M_0}$$
$$\frac{\partial^2 \Phi}{\partial y_1^{*2}} + \frac{\partial^2 \Phi}{\partial y_3^{*2}} + \left(\frac{k_1^* M_0}{\beta^2}\right)^2 \left(1 - \frac{1}{\Theta^2}\right) \Phi = 0 \qquad (2)$$

introducing Graham's gust parameter $\Theta = k_1^* M_0/(k_2^* \beta)$. The associated boundary conditions for a somewhat conventional origin at the center-chord are

$$\frac{\partial \Phi}{\partial y_3^*} = \frac{-c\tilde{w}(k_1, k_2)}{2\beta}, \qquad y_3^* = 0 \qquad -1 \le y_1^* \le 1$$
$$\Delta\left[\frac{\partial \Phi}{\partial y_1^*} - i\frac{k_1^*}{\beta^2}\Phi\right] = 0, \qquad y_3^* = 0 \qquad y_1^* \ge 1$$

and the disturbance pressure follows with a similar factorization $p'_\phi = p(y_1, y_3)\, e^{i(k_2 y_2 - \omega t)}$. The induced unsteady lift $\tilde{\ell}$ or pressure jump is just twice the disturbance pressure on the plate surface because of the phase opposition between both sides of the plate. Depending on gust parameter, eq. (2) is usually of hyperbolic nature and the gust is therefore said supercritical (subcritical gusts do not radiate efficiently for observer in the mid-span plane). Resorting to Schwarzschild's technique, the unsteady lift is found as $\tilde{\ell} = \tilde{\ell}_1 + \tilde{\ell}_2$, with

$$\tilde{\ell}_1(y_1^*, y_2^*, \omega) = \frac{-2\rho_0 U_0 \tilde{w} e^{i\pi/4}}{\sqrt{\pi(k_1^* + \beta^2\bar{\kappa})(1 + y_1^*)}} e^{i(\bar{\kappa} - M_0\bar{\mu})(1+y_1^*)} e^{ik_2^* y_2^*}$$

$$\tilde{\ell}_2(y_1^*, y_2^*, \omega) = \frac{2\rho_0 U_0 \tilde{w} e^{i\pi/4}}{\sqrt{2\pi(k_1^* + \beta^2\bar{\kappa})}} e^{i(\bar{\kappa} - M_0\bar{\mu})(1+y_1^*)} \times \{1 - (1-i)E[2\bar{\kappa}(1 - y_1^*)]\}$$

where $\bar{\kappa} = \sqrt{\bar{\mu}^2 - (k_2^*/\beta)^2}$, $\bar{\mu} = k_1^* M_0/\beta^2$ and E is the Fresnel integral defined as [1]

$$E(\xi) = \int_0^\xi \frac{e^{it}}{\sqrt{2\pi t}}\, dt = C_2(\xi) + iS_2(\xi)$$

3.2 Principle, assumptions and developments

Since most realistic configurations involve overlapping arrangements between the wing and the flap, the modelling is based on two plates with arbitrary relative positionings. The wing is considered as a semi-infinite plate whereas the flap is a finite-chord plate. Most of the models assume compact cases, *id est* when the parameters d and h in figure 5 verify $kd \ll 1$, $kh \ll 1$ and $kc \ll 1$, which corresponds to the spectral bandwidth below 500 Hz in the experiments. Among those configurations, the most pronounced coupling between both surfaces occurs with a significant overlap. As a result, the unsteady pressure on each surface combines the unsteady lift induced by the oncoming aerodynamic disturbances and the acoustic pressure due to the multiple scattering. The analytical model is aimed at reproducing as accurately as possible this combination on the basis of parallel rigid plates with zero thickness.

For the scattering of the flap noise due to the impingement of turbulence, the first iteration procedure is described as follows. It is first calculated the unsteady lift distribution on the flap surfaces by using Amiet's linearized unsteady aerodynamic theory based on Schwarzschild's technique. The equivalent dipole source distribution $\tilde{\ell}(y_1^*)$ is discretized and the scattering of each source point by the trailing-edge of the wing is calculated using the half-plane Green's function with uniform flow. When the direct flap source radiation is subtracted, the solution provides a first evaluation of the pressure jump $\Delta P_W^{(1)}$ over the wing-plate, which is considered as a secondary source distribution, back-scattered by the flap airfoil also according to the half-plane Green's function. The deduced flap pressure jump $\Delta P_F^{(1)}$ comes to correct the unsteady lift distribution given by Amiet's theory as $\tilde{\ell} + \Delta P_F^{(1)}$. Solving again the problem until convergence will tend to the true values of ΔP_W and ΔP_F. The same procedure can be applied to trailing-edge noise sources to obtain an estimate of the total far-field noise.

The two-dimensional reduction of the half-plane Green's function for the convected Helmholtz equation has been de-

rived by Jones [7] and readdressed by Rienstra [11]. Calculations have been made from the MacDonald's formulation [8] of the three-dimensional half-plane Green's function without flow. It reads

$$G^{1/2}(\mathbf{x},\mathbf{y},\omega) = \frac{-ik}{\pi} \times \left\{ \int_{-\infty}^{\xi_1} \bar{K_1}(ikR\cosh\xi)\, d\xi + \int_{-\infty}^{\xi_2} \bar{K_1}(ikR'\cosh\xi)\, d\xi \right\} \quad (3)$$

where $\bar{K_1}$ is the complex conjugate of the modified Bessel function of the second kind [1] and R and R' are the distance observer/source and observer/image of the source by the plane, respectively. After adding a uniform flow in the e_1-direction, the Green's function reads

$$G^{1/2}_{M_0}(\mathbf{x},\mathbf{y},\omega) = \frac{-ik}{\pi} e^{i\frac{kM_0}{\beta^2}(x_1-y_1)} \times \left\{ \int_{-\infty}^{u_1} \frac{\bar{K_1}(iKR^*\sqrt{1+u^2})}{\sqrt{1+u^2}}\, du + \int_{-\infty}^{u_2} \frac{\bar{K_1}(iKR'^*\sqrt{1+u^2})}{\sqrt{1+u^2}}\, du \right\}$$

with $K = k/\beta$ and R^* and R'^* the distances R and R' corrected for the presence of the flow. The far-field pressure is then calculated by multiplying the unsteady lift $\tilde{\ell}$ by the analytical gradient of the Green's function $\nabla G^{1/2}_{M_0}$ and numerically integrated on the flap surface following the aforementioned procedure.

3.3 Sample results and comparisons

The model has been tested and compared with the experiments. For the first calculations, the flap has been discretized as about 30 point sources. The calculations were performed for a single-frequency gust, and the procedure was carried out for several frequencies in order to estimate the qualitative behaviour on the flap surface as well as in the far-field. The time of calculation is of two seconds per point source per complete iteration. For a convergence ratio of 1 %, the modelling needs only 3 or 4 iterations to converge, for frequencies above 1 kHz.

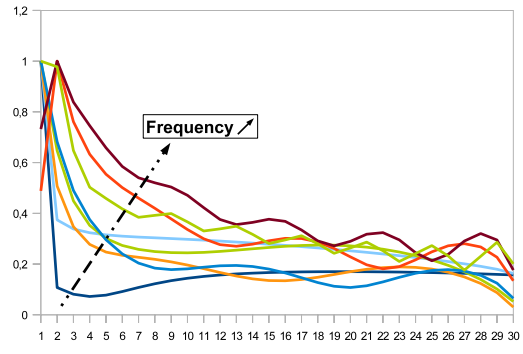

Figure 6: Source distribution resulting from the iterative scattering model between 500 to 12,500 kHz. Configuration 4, 50 m/s.

The first validation was to verify the pattern of the normalized unsteady lift and its evolution during the iterations. Figure 6 is a plot of what is provided in configuration 4 at 50 m/s, for frequencies ranging from 500 to 12,500 Hz. Similarities with the amplitude of the wall-pressure power spectral density (PSD) are found in the experiments, although the statistics of the gusts are not accounted for yet.

Moreover, the calculation of the scattering of flap sources by the wing-plate half-plane is performed at the last iteration according to the distribution of dipoles provided in figure 6. This is aimed at getting the far-field directivity pattern and predicted sound pressure levels. The data can be plotted as polar colour maps (figure 7) to easily compare to the experimental polar diagram of directivity, or as spectra. The main variations of the directivity pattern predicted by the model appear to agree with the total far-field pressure measurements with few differences which can be caused by the integration of the experimental data on a bandwidth of 400 Hz around the frequency of the calculation (4 kHz).

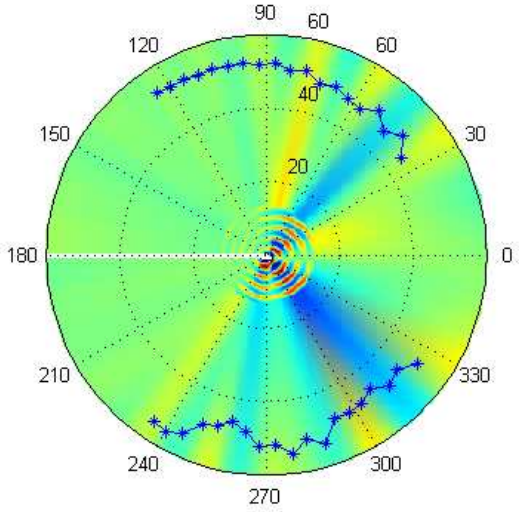

Figure 7: Comparison of directivity between the analytical modelling (colour polar map) and the experiments (polar diagram) at 4 kHz. Configuration 4, 50 m/s.

4 Conclusion

Some experiments have been performed on a simplified wing/flap system in order to provide a reliable database for the understanding of the interactions between two bodies in various arrangements. The study revealed interesting configurations with strong or weak coupling as well as source/scattering screen behaviour. The last has been used in the development of an analytical model involving two rigid plates in an overlapping configuration, with no hypothesis on the dimensions relationship (like compactness). This model is based on the two-dimensional half-plane Green's function in presence of a uniform flow but it can be extended to three-dimensional problems. The iterative procedure leads to the study of coupled bodies and gives interesting results therefore. However, the statistics of the gusts and the response of each body still needs being implemented. Moreover, alternative analytical approaches from the literature will be assessed and compared to the present work (Howe's overlapping theory [5] for instance).

Acknowledgments

The authors are grateful to the experimental team of Centre Acoustique at ECL, especially E. Jondeau, P. Souchotte and J.M. Perrin for their great help in preparing and acquiring the experiment series; as well as ONERA partner people

involved in source localization tests. They also thank EC for supporting VALIANT project which permits this academical study.

References

[1] M. Abramowitz, I.A. Stegun, "Handbook of Mathematical Functions", *Dover, New York* (1970)

[2] R.K. Amiet, "Acoustic Radiation from an Airfoil in a Turbulent Stream", *Journ. Sound and Vib.* **41**(4), 407-420 (1975)

[3] R.K. Amiet, "Refraction of Sound by a Shear-Layer", *AIAA* 15^{th} *Aero. Scien. Meet.*, paper 77-54, Los Angeles, CA (1977)

[4] J.C. Bruyère, M. Vallet, "Évolution des indices acoustiques autour de l'Aéroport de Lyon Saint-Exupéry entre 2002 et 2008", *ODESA Report* (2009)

[5] M.S. Howe, "The Aerodynamic Noise of a Slot in an Airfoil", *Aeron. Res. Coun.*, R&M No.3830 (1978)

[6] M.S. Howe, "Aerodynamic Sound Generated by a Slotted Trailing-Edge", *Proc. Roy. Soc. Lond.* **373**, 235-252 (1980)

[7] D.S. Jones, "Aerodynamic Sound due to a Source Near a Half-Plane", *Journ. Inst. Maths Applics* **9**, 114-122 (1972)

[8] H.M. MacDonald, "A Class of Diffraction Problems", *Proc. Lond. Math. Soc.* **2**(14) (1975)

[9] A. Oberai, F. Roknaldin, T.J.R. Hughes, "Computation of Trailing-Edge Noise Due to Turbulent Flow over an Airfoil", *AIAA Journal* **40**(11), 2206-2216 (2002)

[10] S. Pérennès, "Caractérisation des sources de bruit aérodynamique à basses fréquences de dispositifs hypersustentateurs", *ECL PhD thesis* **99-32**, Lyon (1999)

[11] S.W. Rienstra, "Sound Diffraction at a Trailing-Edge", *Journ. Fluid Mech.* **108**, 443-460 (1981)

[12] R.H. Schlinker, R.K. Amiet, "Refraction of Sound by a Shear-Layer – Experimental Assessment", *AIAA* 5^{th} *Aeroac. Conf.*, paper 79-0628, Seattle, WA (1979)